

Influence of molecular orientation on the coupling of surface plasmons to excitons in semitransparent inverted organic solar cells

Cite as: Appl. Phys. Lett. **106**, 083303 (2015); <https://doi.org/10.1063/1.4913846>

Submitted: 09 December 2014 . Accepted: 18 February 2015 . Published Online: 25 February 2015

Mark Gruber, Michael Mayr, Thomas Lampe, Björn-Christoph Gallheber, Bert J. Scholz, and Wolfgang Brütting



View Online



Export Citation



CrossMark

ARTICLES YOU MAY BE INTERESTED IN

[Determination of molecular dipole orientation in doped fluorescent organic thin films by photoluminescence measurements](#)

Applied Physics Letters **96**, 073302 (2010); <https://doi.org/10.1063/1.3309705>

[Extracting the emitter orientation in organic light-emitting diodes from external quantum efficiency measurements](#)

Applied Physics Letters **105**, 043302 (2014); <https://doi.org/10.1063/1.4891680>

[High-efficiency fluorescent organic light-emitting diodes enabled by triplet-triplet annihilation and horizontal emitter orientation](#)

Applied Physics Letters **105**, 183304 (2014); <https://doi.org/10.1063/1.4901341>

Lock-in Amplifiers

... and more, from DC to 600 MHz



Influence of molecular orientation on the coupling of surface plasmons to excitons in semitransparent inverted organic solar cells

Mark Gruber,^{a)} Michael Mayr, Thomas Lampe, Björn-Christoph Gallheber, Bert J. Scholz, and Wolfgang Brütting^{b)}

Institute of Physics, University of Augsburg, 86135 Augsburg, Germany

(Received 9 December 2014; accepted 18 February 2015; published online 25 February 2015)

We investigate the coupling between surface plasmons and excitons for different donor materials in semitransparent organic solar cells. Surface plasmons can be excited at the interface between the semitransparent anode and the surrounding dielectric medium in Kretschmann configuration, if the resonance condition for wavelength and angle is fulfilled. In solar cells with nearly upright standing diindenoperylene donor molecules in close proximity to the metal, this can lead to an enhancement in photo-current. By contrast, for cells with dibenzo-tetraphenyl-periflanthen as donor, the lying orientation of molecules is unfavorable for coupling to surface plasmons. In this case, the excitation of surface plasmons acts like a parasitic absorption and reduces the photo-current. © 2015 AIP Publishing LLC. [<http://dx.doi.org/10.1063/1.4913846>]

Organic photovoltaic cells (OPVCs) have recently surmounted the 10% mark¹ in power conversion efficiency and are close to the edge of being commercialized. This goal was reached by introducing new donor and acceptor materials with increased absorption strength and a more favorable energetic alignment. To further increase thin film solar cell efficiency—organic as well as inorganic PVCs—research directs its focus more and more on techniques for third generation photovoltaics. In this context, light management, spectral conversion, and multi-junction concepts are used to push the efficiency limit beyond the Shockley-Queisser limit for single junctions.^{2,3} This work focuses on another promising concept to increase solar cell efficiency by transferring energy from surface plasmons (SPs) to molecules accompanied by additional exciton generation, leading to increased short-circuit current under preserved open-circuit voltage and fill factor.^{4–6}

Due to very thin films and short exciton diffusion lengths, absorption is well below unity in organic photovoltaics. An increase in absorption over a broad spectral range can be achieved by the use of SP active structures, like corrugated metal electrodes and metallic nanoparticles.^{7–9} To gain from this additional absorption, it is necessary to transfer energy from SPs to molecules by generating excitons which can contribute to the short-circuit current density (j_{SC}) of the OPVC. Hayashi *et al.*¹⁰ and Kume *et al.*¹¹ showed for single layer semitransparent organic solar cells that it is possible to increase the photo-current in the presence of an SP resonance. They used Copper-Phthalocyanine (CuPc) as absorber and aluminum and silver as electrodes which serve as exciton dissociation centers by forming Schottky junctions to CuPc. The SP is excited at the interface between the top silver electrode and air. Here, we investigate much more efficient molecular donor/acceptor (D/A) solar cells based on perylene derivatives and a fullerene derivative as photo-active layers. To check the dependence of the coupling behaviour of SPs to excitons on

transition dipole moment orientation, identically processed inverted cells with two different donor materials—diindenoperylene (DIP) and dibenzo-tetraphenyl-periflanthen (DBP)—are compared. While DIP crystallizes with nearly upright standing molecules^{12,13} on the underlying Phenyl-C₆₁-butyric acid methyl ester (PCBM) acceptor, DBP shows—due to the sterically unfavorable four rotatable phenyl rings—a disordered growth behaviour with mainly lying molecules.^{14,15}

The investigated OPVC stack is shown in Figure 1. For selective electron extraction, the transparent indium-tin oxide (ITO) electrode is covered with a thin layer of polyethylenimine ethoxylated (PEIE).¹⁶ Hole selectivity is granted by using MoO₃ between the active layers and the semitransparent silver anode. The thicknesses of the donor layers DIP and DBP is 20 nm each. This is necessary for comparability and to grant the diffusion of possibly generated excitons by SPs to the D/A interface within the exciton diffusion length. It should be mentioned that the thickness is not optimized for the cavity effect, i.e., the main exciton generation by direct light absorption is not at the D/A interface. Due to that fact, the power conversion efficiency cannot be compared with published data of their non-inverted pendants.^{17,18} In

Dielectric medium	LiF (0,50,100,150 nm)	SP
	Ag (20,100 nm)	
Anode	MoO ₃ (10 nm)	
	DIP/DBP (20 nm)	
Active layer	PCBM (46 nm)	
	PEIE (11 nm)	
Cathode	ITO (145 nm)	
	Glas	

FIG. 1. Stack of the inverted semitransparent and reference organic solar cells with ITO/PEIE serving as cathode, PC₆₁BM as acceptor, DIP or DBP as donor, MoO₃/Ag as anode, and LiF effective dielectric medium in combination with surrounding air to shift the angular position of the excited SP (indicated by red plus and minus symbols).

^{a)}Email: Mark.Gruber@physik.uni-augsburg.de

^{b)}Email: Wolfgang.Brueetting@physik.uni-augsburg.de

particular, a reduction in j_{SC} compared to the published devices can be observed for these OPVCs (see Figure 2), while the loss in fill factor can be explained by increased leakage currents and is of minor impact. Due to the use of PCBM instead of C_{60} , the open-circuit voltage (V_{OC}) is about 0.1 V higher than in non-inverted devices.¹⁹ The reference devices with 100 nm Ag show slightly increased j_{SC} as well as V_{OC} . While the increased j_{SC} is a result of the fully reflecting back electrode, higher V_{OC} is not obvious. This is mainly due to a variation of leakage currents and with that of V_{OC} in different devices. The presented j - V -characteristics correspond to the OPVCs, where the spectral photo-current was measured (Figures 4 and 5) but are not representative in terms of V_{OC} .

Figure 3 shows the setup for simultaneous measurement of reflectance and photo-current. To prove the angular position of the SP, the samples were measured in reflectance with a green laser (532 nm) using a photo-diode as detector. Exciting SPs directly by light requires a glass prism to fulfill the energy-momentum conservation (setup in Kretschmann configuration²⁰). Additionally, there is a polarizer to switch between s- and p-polarization of the incident laser beam. The influence of the SP on the solar cell characteristics can be detected by simultaneously measuring reflectance and photo-current, while sample and photo-detector are rotated on a Θ - 2Θ stage.

Due to high refractive indices of the photo-active and carrier-selective layers, the SP is located between silver and the surrounding dielectric medium (see Figure 1). To get an influence of the SP on the donor, it has to be in reach of the evanescent field of the SP. Therefore, the inverted architecture was chosen, where the donor is placed near the back electrode. To verify and demonstrate the location of the SP, the refractive index of the surrounding medium is varied by using different layer thicknesses of lithium fluoride (LiF), namely, 0, 50, 100, and 150 nm (nominal thickness). As the evanescent field of the SP partially penetrates the LiF layer and reaches air, the effective refractive index of the dielectric medium changes with varying LiF thickness and leads to a shift of the SP resonance. The reference devices with the same active layer stack do not show SP excitation by the incident laser beam, as the 100 nm silver anode is too thick for penetration of the evanescent field.

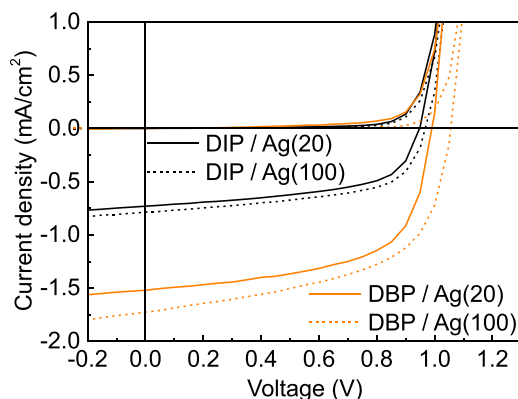


FIG. 2. j - V -characteristics of the reference devices (100 nm Ag) and the OPVCs (20 nm Ag) with 0 nm LiF under simulated AM1.5 g illumination (stack see Figure 1). The reduced j_{SC} in the devices with thin silver Anode results from the semitransparency.

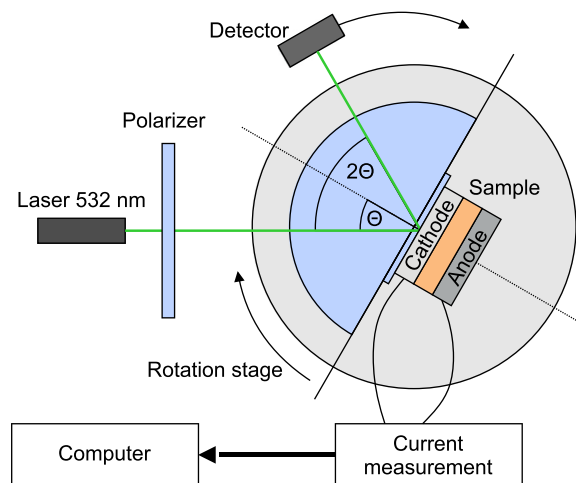


FIG. 3. Sketch of the Kretschmann configuration setup for angle dependent reflectance and photo-current measurements of the presented OPVCs (see Figure 1). To have an effect on both donor materials (DIP and DBP), the laser wavelength was chosen to be 532 nm.

Figures 4 and 5 show the results of optical simulations and measurements of OPVCs with DIP and DBP as donor material, respectively, and the different LiF layer thicknesses as well as the reference devices. For a better understanding of the features in the measured data, reflectance and absorbance of all samples were simulated with a self-developed simulation tool including birefringence of the two donor materials (for used n - and k -values and details concerning the simulation see supplementary material²¹) for a wavelength of 532 nm. The subfigures “(a) and (b)” and “(e) and (f)” of Figures 4 and 5 show the simulated reflectance of the whole stack and the sum of the absorbance of donor and acceptor in p- and s-polarization, respectively. The p-polarized simulations exhibit a drop in reflectance in the angular range of SP excitation above the critical angle of glass for total internal reflection (42°), while the absorbance shows a drop for the sample without LiF and almost no change for the one with a thin LiF layer. Thicker LiF layers actually lead to an increased absorption in the photo-active layers. These variations in amplitude—despite the fact that the angular position varies—can be attributed to interference effects of the incident light with the electric field of the excited SP. In s-polarization, there is no SP excitation present, though a pronounced peak in reflectance is observed for a nominal 150 nm thick LiF layer. This increase of reflectance is attributed to an upcoming wave-guided mode in LiF, which also leads to a drop in absorption.

The subfigures “(c) and (d)” and “(g) and (h)” of Figs. 4 and 5 show the measured reflectance and the photo-current for both donors. Both are normalized to the simulated data at 8° (lower limit of rotation angle, because of beam stop by the detector in reflectance measurements). The photo-current of the reference cells follows mainly the shape of the simulated absorbance. For angles higher than about 60° – 70° ; however, the curve begins to decline rapidly as a result of the broadened laser spot exceeding the OPVC pixel size (for a comparison between simulated absorbance and measured photo-current to illustrate the geometrical influence, see supplementary material²¹). All these effects are present in the

semitransparent samples too. Additionally, total internal reflection at 42° leads to a kink in photo-current due to the partially transparent anode.

The position of the SP excitation in the measured p-polarized reflectance data fits quite well to the simulated curves for DIP and DBP as donor. Therefore, the used thicknesses for LiF in simulated data are adapted to the most appropriate fit considering reflectance and absorption data in s- and p-polarization, respectively. However, for DIP the trend of the SP excitation amplitude in the reflectance data (Figure 4(e)) is contrary to that of the simulation (Figure 4(a)). This effect is attributed to the presence of SP coupling to excitons, as the DBP containing device (Figure 5) does not show any severe deviations from the simulation.

The effect on photo-current for DIP containing devices can be seen in Figures 4(g) and 4(h). In the case of p-polarized incident light, the photo-current shows—dependent of the LiF thickness—enhancement in the angular range of the SP resonance (see also section “geometrical factor” in

the supplementary material²¹). This can be seen as proof for efficient coupling of SPs to upright standing molecules. However, for the thickest LiF layer in s-polarization, instead of increasing j_{SC} , the trapped light in wave-guided modes leads to a pronounced decrease in current in a small angular range.

Figures 5(c) and 5(d) show the measured reflectance data of the OPVCs containing DBP as donor material. The trend is comparable to the samples with DIP, while the overall reflectance level is lower due to the stronger absorption of DBP.¹⁸ By contrast, the photo-current in p-polarization reveals a clearly different trend (compare Figures 4(g) and 5(g)). While the DIP samples profit from SP excitation, the samples with DBP clearly follow the simulated drop in photocurrent. This is attributed to the unfavorable orientation of DBP molecules for coupling of SPs to excitons. Additionally, wave-guided modes in s-polarization lead to a pronounced reduction of photo-current in the angular range of excitation, similar to the behavior in DIP containing OPVCs.

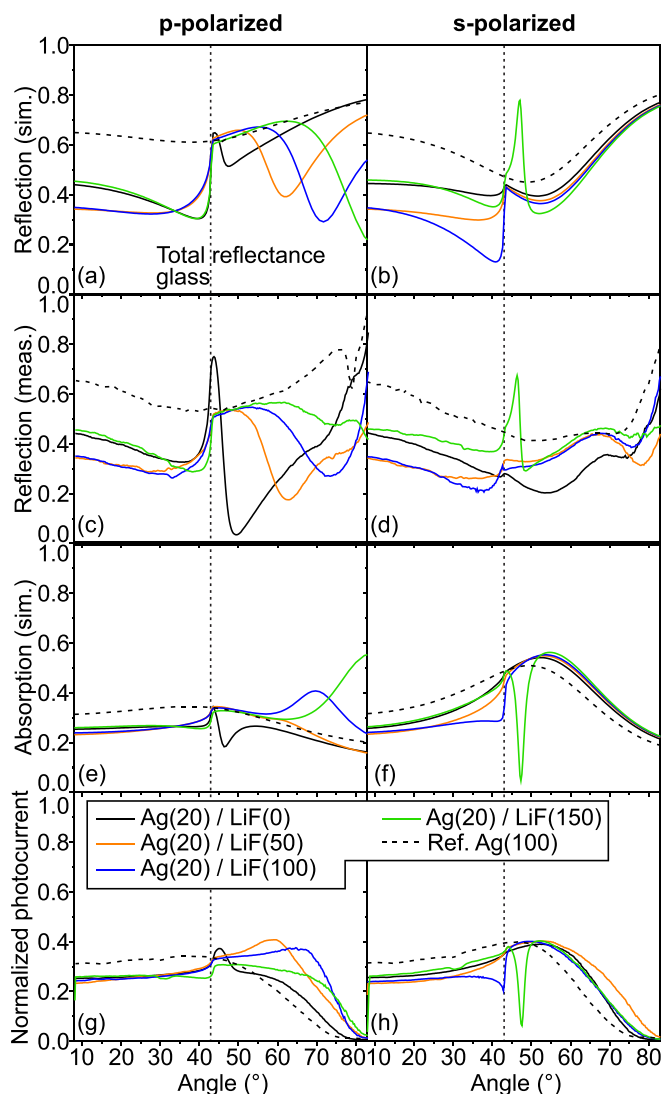


FIG. 4. (a) and (b) simulated and (c) and (d) measured reflectance data and (e) and (f) simulated absorbance of the absorber layers and (g) and (h) photo-current measurements for OPVCs containing DIP as donor material in s- and p-polarization, respectively. The simulation fits best to the experimental data using 55, 90, and 165 nm LiF layer thickness, respectively. The legend indicates the nominal thickness of LiF.

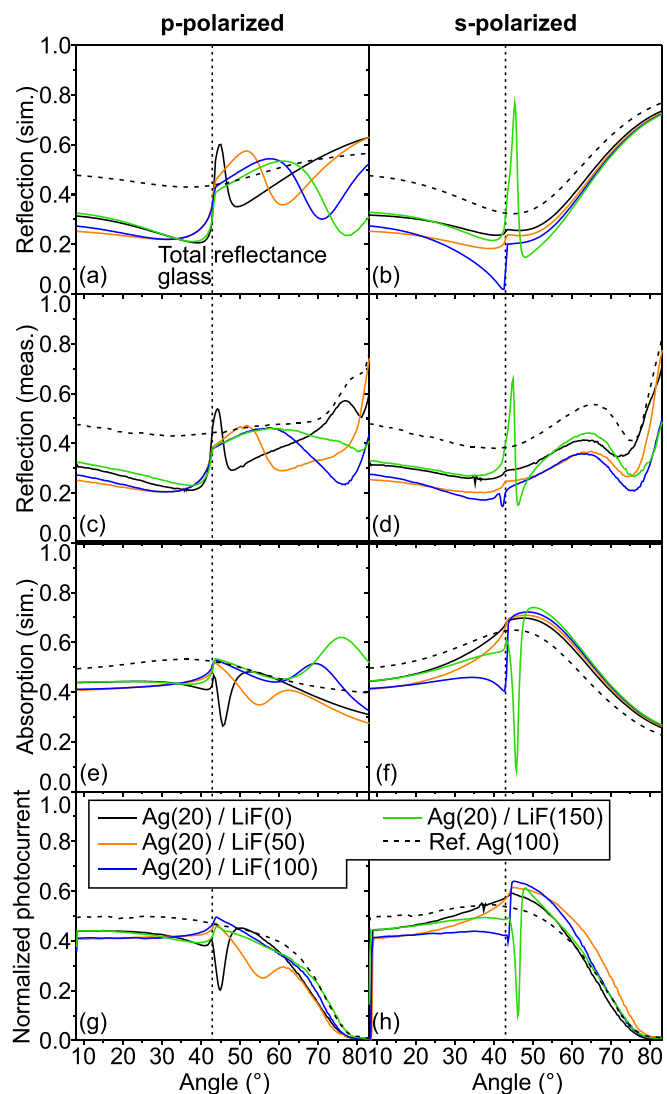


FIG. 5. (a) and (b) simulated and (c) and (d) measured reflectance data and (e) and (f) simulated absorbance of the absorber layers and (g) and (h) photo-current measurements for OPVCs containing DBP as donor material in s- and p-polarization, respectively. The simulation fits best to the experimental values using the LiF layer thicknesses given in the legend.

Thus, the use of two different types of molecular donors—concerning the orientation of their transition dipole moment—allows to demonstrate the positive effect of SP excitation on photo-current in OPVCs with upright oriented donor molecules. Wave-guided modes outside the main OPVC stack are not able to couple to any transition dipole moment orientation.

These results show the potential benefits of SPs on solar cell performance, at least on upright oriented transition dipole moments. Due to low efficiency and the necessity of a glass prism or micro lens array, single junctions with good absorbers will always beat this concept in terms of application relevance. However, this work clearly demonstrates the requirements of molecular orientation in solar cells for gaining energy from SPs. These findings are, in principle, also valid for photovoltaics introducing periodically corrugated electrodes as grating for SP coupling instead of a prism coupler, though there may be slightly different requirements on the molecular orientation depending on the detailed specification of the integrated grating in terms of shape and position in the layer stack. With this concept, also the light loss by semi-transparency can be overcome, as the transfer of momentum to or from the grating to incident photons can shift the dispersion relation in a way that SPs are excitable without the necessity of a surrounding medium with low dielectric constant.

The grating concept may have an advantage in special applications, where, e.g., high currents under certain angles are required. For direct illumination, i.e., standard applications, devices with good absorbers exhibiting high charge carrier mobilities will be the more economic choice, especially concerning fabrication complexity.

This work was supported by the German Research Foundation (DFG) within the priority program SPP1355 (Elementary Processes of Organic Photovoltaics) as well as the Bavarian State Ministry of Science, Research and the Arts within the collaborative research network “Solar Technologies

go Hybrid” (SolTech). We want to thank Christian Mayr for support during angular dependent measurements and help with determination of optical constants.

- ¹J. You, L. Dou, K. Yoshimura, T. Kato, K. Ohya, T. Moriarty, K. Emery, C.-C. Chen, J. Gao, G. Li, and Y. Yang, *Nat. Commun.* **4**, 1446 (2013).
- ²G. F. Brown and J. Wu, *Laser Photon. Rev.* **3**, 394 (2009).
- ³W. Shockley and H. J. Queisser, *J. Appl. Phys.* **32**, 510 (1961).
- ⁴A. P. Kulkarni, K. M. Noone, K. Munechika, S. R. Guyer, and D. S. Ginger, *Nano. Lett.* **10**, 1501 (2010).
- ⁵H. Atwater and A. Polman, *Nat. Mater.* **9**, 205 (2010).
- ⁶A. Polman and H. Atwater, *Nat. Mater.* **11**, 174 (2012).
- ⁷A. J. Morfa, K. L. Rowlen, T. H. Reilly, M. J. Romero, and J. van de Lagemaat, *Appl. Phys. Lett.* **92**, 013504 (2008).
- ⁸V. E. Ferry, M. A. Verschuuren, H. B. T. Li, E. Verhagen, R. J. Walters, R. E. I. Schropp, H. A. Atwater, and A. Polman, *Opt. Express* **18**, A237 (2010).
- ⁹S. Y. Chou and W. Ding, *Opt. Express* **21**, A60 (2013).
- ¹⁰S. Hayashi, K. Kozaru, and K. Yamamoto, *Solid State Commun.* **79**, 763 (1991).
- ¹¹T. Kume, S. Hayashi, H. Ohkuma, and K. Yamamoto, *Jpn. J. Appl. Phys., Part 1* **34**, 6448 (1995).
- ¹²A. C. Dürr, F. Schreiber, M. Münch, N. Karl, B. Krause, V. Kruppa, and H. Dosch, *Appl. Phys. Lett.* **81**, 2276 (2002).
- ¹³A. C. Dürr, F. Schreiber, K. A. Ritley, V. Kruppa, J. Krug, H. Dosch, and B. Struth, *Phys. Rev. Lett.* **90**, 016104 (2003).
- ¹⁴D. Yokoyama, Z. Q. Wang, Y.-J. Pu, K. Kobayashi, J. Kido, and Z. Hong, *Sol. Energy Mater. Sol. Cells* **98**, 472 (2012).
- ¹⁵Y.-Q. Zheng, Z. W. J. Potscavage, T. Komino, M. Hirade, J. Adachi, and C. Adachi, *Appl. Phys. Lett.* **102**, 143304 (2013).
- ¹⁶Y. Zhou, C. Fuentes-Hernandez, J. Shim, J. Meyer, A. J. Giordano, H. Li, P. Winget, T. Papadopoulos, H. Cheun, J. Kim, M. Fenoll, A. Dindar, W. Haske, E. Najafabadi, T. M. Khan, H. Sojoudi, S. Barlow, S. Graham, J.-L. Brédas, S. R. Marder, A. Kahn, and B. Kippelen, *Science* **336**, 327 (2012).
- ¹⁷J. Wagner, M. Gruber, A. Hinderhofer, A. Wilke, B. Bröker, J. Frisch, P. Amsalem, A. Vollmer, A. Opitz, N. Koch, F. Schreiber, and W. Brütting, *Adv. Funct. Mater.* **20**, 4295 (2010).
- ¹⁸S. Grob, M. Gruber, A. N. Bartynski, U. Hörmann, T. Linderl, M. E. Thompson, and W. Brütting, *Appl. Phys. Lett.* **104**, 213304 (2014).
- ¹⁹C.-W. Chu, V. Shrotriya, G. Li, and Y. Yang, *Appl. Phys. Lett.* **88**, 153504 (2006).
- ²⁰E. Kretschmann, *Opt. Commun.* **6**, 185 (1972).
- ²¹See supplementary material at <http://dx.doi.org/10.1063/1.4913846> for details on simulation and n- and k-values of the used materials.